Finite Element Prediction of Elastic Recoil after Stent Implantation

Laroche, Denis; Mora, Vincent; Delorme, Sébastien; Debergue, Patricia; Anderson, Todd; Diraddo, Robert

Publisher's version / Version de l'éditeur:

8th International Symposium on Computer Methods in Biomechanics and Biomedical Engineering (CMBBE 2008) [Proceedings], pp. 1-6, 2008-02-27

FINITE ELEMENT PREDICTION OF ELASTIC RECOIL AFTER STENT IMPLANTATION

D. Laroche[1], V. Mora[1], S. Delorme[1], P. Debergue[1], T. Anderson[2] and R. DiRaddo[1]

1. ABSTRACT

A finite element model for simulating stent implantation into coronary arteries is presented. The model computes large deformations and contact mechanics to predict artery lumen patency, as well as stress and strain distribution in the arterial wall, after balloon inflation and deflation for a specific stent and inflation pressure. Unconfined stent deployment in air was measured experimentally and simulated for two stainless steel stents. Model predictions showed excellent agreement with experimental results. Stent deployment in coronary arteries was also validated using in-vivo pre- and post-intervention IVUS images from three patients who underwent stent implantation. Lumen patency after immediate elastic recoil is predicted. Discrepancy between predicted and measured post intervention lumen may be due to the lack of personalized arterial wall mechanical properties.

2. INTRODUCTION

Percutaneous Coronary Intervention (PCI) is the most common intervention for restoring adequate blood flow in stenosed arteries. In most cases, a stent is deployed and permanently implanted to mechanically dilate the artery and maintain lumen patency. The intervention strategy, including stent selection, its positioning and balloon inflation pressure, is typically determined by angiographic images, patient clinical information and clinician's experience. The most frequent complication of PCI, restenosis, is an excessive repair reaction of the arterial wall related to its mechanical damage during the intervention. Whether because of patients comeback after 6 months for target vessel revascularization or because of the use of expensive drug-eluting stents, restenosis increases the total cost of this intervention.

Few research groups have attempted to simulate PCI with numerical or analytical models to predict its outcome [1-6]. Finite element simulation of stent deployment in stenosed arteries has been proposed as a tool for stent design. Our group has proposed finite element modeling of stent implantation with artery model reconstruction from patient-specific intra-vascular ultra-sound (IVUS) imaging to assist clinicians in the selection of appropriate intervention strategy [1,6]. The model computes large deformations and contact mechanics in a fully implicit algorithm to solve balloon-stent-artery interactions that occur during stent deployment inside the stenosed artery. It predicts resulting artery lumen reopening, including stress and strain distribution in the arterial wall, for a specific stent and balloon inflation pressure.

---

[1]Researcher, Industrial Materials Institute, National Research Council Canada, Boucherville, QC, Canada
[2]Professor, Department of Medicine, University of Calgary, Calgary, AB, Canada

In this work, an elasto-plastic model is proposed for the stent to predict the immediate elastic recoil after balloon deflation. The stent model is validated using unconfined stent deployment experiments in air as well as using IVUS images from three patients who underwent direct stenting.

3. BALLOON AND STENT MODEL

PCI are typically performed using balloon deployable stents consisting of a stent mounted onto a pre-wrapped balloon. The balloon is welded onto a catheter and is made of hyperelastic polymers. Its thin walls were modeled with membrane elements. Strain hardening of the polymer was modeled using the Ogden constitutive equation with two terms [7]. The strain energy W of the model is given by:

$$W = \sum_{i=1}^{2} \frac{\mu_i}{\alpha_i} \left(\lambda_1^{\alpha_i} + \lambda_2^{\alpha_i} + \lambda_3^{\alpha_i} - 3 \right) \quad [1]$$

where λ_1, λ_2 and λ_3 are the principal stretch ratios and μ_i and α_i are the model constants with the following values [7]: $\mu_1 = 154$ MPa, $\alpha_1 = 0.2$, $\mu_2 = 13$ MPa, $\alpha_2 = 12$.

Coronary stents are made of thin metal struts that exhibit elasto-plastic behaviour and deform mostly in bending. They were modeled with incompressible hexahedral elements and the Prandtl-Reuss constitutive equation. As suggested by [8,9], the model was generalized to finite deformations using additive decomposition of the Almansi strain tensor. The plastic flow is orthogonal to the Von-Mises yield criterion given by Equation 2 where σ is the deviatoric stress tensor and R is a linear isotropic hardening function given by Equation 3.

$$F(\sigma, R) = \sqrt{\tfrac{3}{2}\sigma : \sigma} - R \leq 0 \quad [2]$$

$$R(p) = R_0 + \kappa p \quad [3]$$

The initial yield stress is R_0, p is the cumulated plastic strain and κ is the hardening parameter. Model constants for stainless steel 316L and cobalt-chromium were fitted from literature data [10,11] and are given in Table 1, where μ is the elastic shear modulus.

	Stainless steel 316L	Cobalt-chromium
μ	37000 MPa	46000 MPa
R_0	350 MPa	600 MPa
κ	950 MPa	1500 MPa

Table 1: Elasto-plastic model constants for stainless steel and cobalt-chromium.

The stent is deployed by applying an internal pressure into the balloon. A multi-body contact algorithm developed for implicit finite element computation [1] is used to model contacts between the balloon folds and the stent struts. It computes continuous collision detections between virtual nodes and surfaces.

4. PATIENT-SPECIFIC ARTERY MODEL

A tetrahedral finite element mesh of the artery segment was created from pre-intervention IVUS pullback images, *a posteriori* sampled at cardiac frequency. Mechanical characterization of arteries has shown high differences between individuals and between artery layers, such as intima, media, adventitia, and plaque components [12,13]. However, to our knowledge, segmentation of inter-layer borders other than lumen-intima and media-adventitia from conventional IVUS images has not yet been reported. Therefore a homogeneous distribution was assumed. The following two-term Mooney-Rivlin constitutive equation, proposed by Ballyk [3], was used:

$$W = c_{01}(I_2 - 3) + c_{20}(I_1 - 3)^2 \qquad [4]$$

where the strain energy W is a function of strain invariants I_1 and I_2 and model constants c_{01} and c_{20}. These constants are obtained by fitting experimental data obtained from the literature [12,13]. Figure 1 shows reported tensile test measurements on human arteries in axial and circumferential directions. Fits for healthy coronary media and iliac atherosclerotic intima layers are also plotted. Proposed averaged model constants for healthy media are c_{01} = 0.001 MPa and c_{20} = 0.004 MPa, and are c_{01} = 0.045 MPa and c_{20} = 3.75 MPa for atherosclerotic intima.

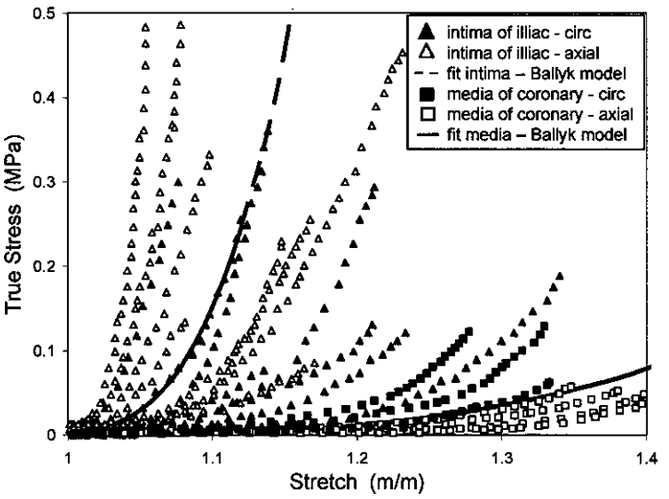

Figure 1: Reported circumferential and axial tensile test data on human arteries. Atherosclerotic iliac intima and healthy coronary media are shown, along with adjusted numerical model.

5. VALIDATION

5.1. Unconfined Stent Deployment

In order to validate the proposed device model, free deployment experiments were conducted for two balloon-deployable stents: a 12-mm long by 3-mm diameter stainless steel Taxus stent (Boston Scientific), and a 20-mm long by 2.5-mm diameter stainless

steel Liberty stent (Boston Scientific). Simulations of stent deployment with balloon inflation were performed for the Taxus and the Liberty stainless steel stents. Figure 2 shows an experimental picture and the predicted balloon-stent shape during deployment of the Taxus stent. Figure 3 shows measured and predicted stent diameter as a function of balloon inflation pressure for the Taxus and Liberty stents. Predictions are in good agreement with measurements, except at the extremities of the Liberty stent.

Experiments Prediction

Figure 2: Experimental and predicted deployment of the Taxus stainless steel stent at balloon pressure of 0.4 MPa.

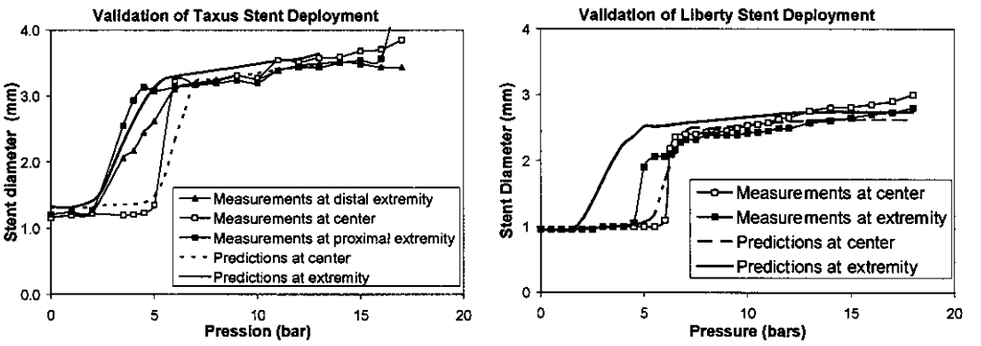

Figure 3: Comparison between predicted and measured stent deployment for the Taxus and the Liberty stents. Stent diameters at its center and extremities are reported as a function of balloon internal pressure.

5.2. In-vivo Validation of PCI

An in-vivo validation of the finite element model was conducted for three patients who underwent a PCI. Table 2 gives intervention information.

	Patient	Artery	Stent	Inflation pressure
A	54 year old female	Mid-LAD	3x12mm Taxus, Bos. Sci.	1,8 MPa
B	57 year old male	Mid-LAD	3.5x18mm Vision, Guidant	1,8 MPa
C	73 year old female	Mid-LCx	2.5x20mm Liberty, Bos. Sci.	1,4 MPa

Table 2: Intervention information for the three in-vivo validation cases.

Finite element meshes of the targeted artery segments were created from pre-intervention IVUS images. Simulations were performed using mechanical properties of healthy coronary media and of atherosclerotic iliac intima. The simulations began with the device in position (before balloon inflation) and ended after complete balloon deflation and immediate recoil of the artery and stent. Figure 4 shows steps during PCI simulation for Patient C using mechanical properties of the atherosclerotic intima.

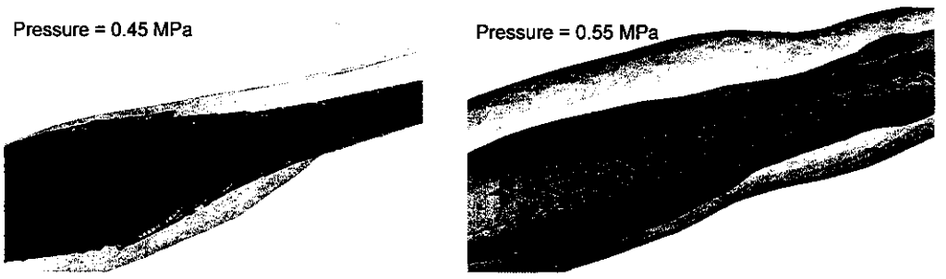

Figure 4: Finite element simulation of PCI for Patient C at 0.45 MPa and 0.55 MPa.

In order to compare the predicted artery shape with the post-intervention images, the two datasets were aligned using the position and orientation of the artery bifurcations. Lumen area was measured on transverse images extracted at proximal, center and distal positions along the stented artery segment, and is plotted in Figure 5. Predicted lumen areas before and after the elastic recoil are also shown, including simulations using properties of healthy coronary media and of atherosclerotic iliac intima.

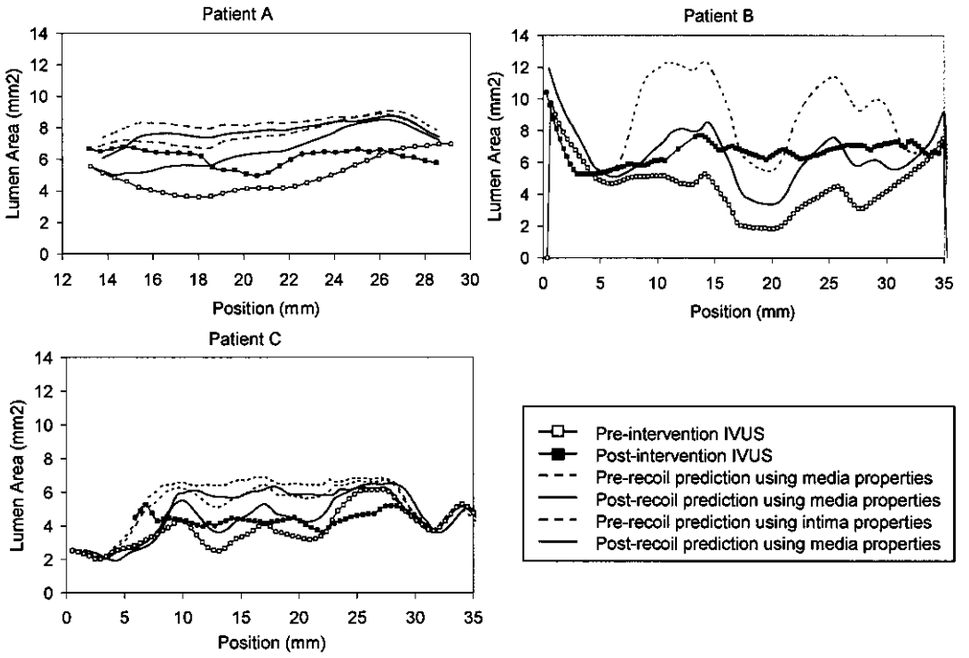

Figure 5: Comparison between predicted and measured artery lumen area for the three patients. Lumen area is plotted as a function of position along artery segment.

When comparing numerical results of lumen cross-sections with post-intervention data, it can be seen that the model better predicts the final lumen area when using atherosclerotic intima properties. In general good correlation is observed. However the measured uniform lumen area along the arteries could not be predicted. This is probably due to the use of a homogeneous rather than a layer-specific model of the arterial wall. The use of image-based tissue classification with IVUS, such as Virtual Histology (Volcano Therapeutics), or the use of CT-scan to discriminate calcium inclusion in the arterial wall, could help improve the accuracy of the simulation results.

6. CONCLUSION

In this work a finite element model for predicting elastic recoil after stent implantation was proposed. The model simulates the deployment of a balloon-deployable stent into a patient-specific artery obtained from conventional IVUS imaging. The deployment mechanics of the balloon-stent model was validated from measurements of unconfined stent deployments in air. An in-vivo validation using pre- and post-intervention medical images from three patients who underwent direct stenting was presented. Prediction of post-intervention lumen area was more accurate in stent extremities than at stent mid-length. The elastic recoil resulting from balloon deflation was clearly observed. The in-vivo validation highlighted the need for improvement of the patient-specific model of the artery.

7. REFERENCES

1. Laroche, D., Delorme, S., Anderson, T. and DiRaddo, R., In-vivo validation of a stent implantation numerical model, Medicine Meets Virtual Reality 14, J.D. Westwood et al. (Eds), Technology and Informatics, 2007, Vol. 125, 265-270.
2. Holzapfel, G.A. et al., A layer-specific three-dimensional model for the simulation of balloon angioplasty using magnetic resonance imaging and mechanical testing, Ann. Biomed. Eng., 2002, Vol. 30, 753-767.
3. Ballyk, P., Intramural stress increases exponentially with stent diameter: a stress threshold for neointimal hyperplasia, J. of Vascular and Intervent. Radiol., 2006, Vol. 17, 1139-1145.
4. Eftaxiopoulos, D.A. and Atkinson, C., A nonlinear, anisotropic and axisymmetric model for balloon angioplasty, Proc. Royal Society, 2005, Vol. 461, 1097-1128.
5. Di Puccio, F. et al., Finite element modelling of balloon angioplasty, Proc. IASTED int. conf., June 2003, Rhodes, Greece, 387-392.
6. Laroche, D., Delorme, S., Anderson, T. DiRaddo, R. Computer Prediction of Friction in Balloon Angioplasty and Stent Implantation. Biomedical Simulation: 3rd Int. Symp, ISBMS, Zurich, Switzerland, 2006, 1-8.
7. Delorme S, Laroche D, DiRaddo R, Buithieu J. Modeling polymer balloons for angioplasty: from fabrication to deployment. Proc Annual Technical Conference (ANTEC), SPE, Chicago, IL, 2004.
8. Simo, J.C. and Ortiz, M., A unified approach to finite deformation elastoplastic analysis based on the use of hyperelastic constitutive equations, Comp. Meth. Appl. Mech. Eng., 1985, Vol. 49, 221-245.
9. Haupt, P., On the concept of an intermediate configuration and its applications to a representation of viscoelastic-plastic material behaviour, Int. J. Plasticity, 1985, Vol. 1, 303-316.
10. Ullmaier, H. and Chen, J., Low temperature tensile properties of steels containing high concentrations of helium, 2003, Vol. 318, 228-233.
11. Davenport, J.C. et al., Retention, British Dental Journal, 2000, Vol. 189, 646-657.
12. Holzapfel, G.H. et al., Anisotropic mechanical properties of tissue components in human atherosclerotic plaques, J. Biomech. Eng., 2004, Vol. 126, 657-665.
13. Holzapfel, G.A., Sommer, G., Gasser, C.T. and Regitnig, P., Determination of layer-specific mechanical properties of human coronary arteries with non-atherosclerotic intimal thickening and related constitutive modeling, American Journal of Physiology, Heart and Circulatory Physilology, 2005, Vol. 289, 2048-2058.